ON THE FLUTTER SPEED OF A ROTOR BLADE IN FORWARD FLIGHT[i]

E. R. Wood[ii], M. A. Couch[iii], and D. Canright[iv]

Naval Postgraduate School
Monterey, California, USA

Abstract

Presented is a theoretical method for determining rotor blade flutter in forward flight and a sample problem that considers coupled bending torsion flutter of a modified UH-60 rotor blade. The theory accounts for the unsteady aerodynamic contribution of the wake below the rotor. This is made possible due to certain simplifying assumptions regarding the rotor's wake. In particular, it is assumed at the onset of flutter that oscillations begin to build up prior to the blade reaching a critical azimuth position, then decay as the blade moves beyond this point. Using the new forward flight lift deficiency function, the authors set up and repeatedly solve the flutter determinant for the blade in the conventional manner (Ref 7) to obtain the blade's flutter speed. For the sample analysis the UH-60 rotor blade is modified to make it "flutter susceptible". This is achieved by moving the chordwise position of the blade's center-of-gravity aft of the quarter chord while keeping its elastic axis at the quarter chord.

Nomenclature

A, $\bar{A}$	aerodynamic terms in flutter equations
a	non-dimensional elastic axis location measured from midchord
b	semi-chord length
$C(k)$	Theodorsen's lift deficiency function
$C(k,h,m)$	Loewy's lift deficiency function
$C'_N(k,h,m)$	finite-wake lift deficiency function,
$C_1(k,\mu,\lambda)$	Shipman-Wood lift deficiency fn. (Ref 4)
D	dissipation function
e	flapping hinge offset from center of rotation
E	elastic (Young's) modulus
F	real part of lift deficiency function
g	blade or wing damping
G	imaginary part of lift deficiency function
h	non-dimensional distance between layers of shed vorticity (wake spacing), $h = 2\pi v/bQ\Omega$
h_n	blade deflection due to n^{th} bending mode
$H_n^{(2)}$	Hankel function (complex Bessel function) of second kind of order n, $H_n^{(2)} = J_n - Y_n$
I_n	generalized mass for n^{th} mode due to torsion
J_n	real part of complex Bessel function of order n
k	reduced frequency, $k = \omega b/v$ (fixed wing), or $k = \omega b/\Omega r$ (rotary wing)
K_n	Southwell coefficient
l	length of beam (semispan of airfoil for fixed wing, or $l = R - e$ for rotary wing)
L_α	aerodynamic lift due to pitch
L_h	aerodynamic lift due to plunge
m	ratio of oscillation frequency to rotational frequency, $m = \omega/\Omega$
M_n	generalized mass of n^{th} mode due to flapwise bending
M_α	aerodynamic moment about elastic axis due to pitch (positive clockwise)
M_h	aerodynamic moment about elastic axis due to plunge
n	revolution number
N	number of wakes for a single-blade rotor
q_n	normal coordinate for n^{th} mode
Q_n	generalized force for n^{th} mode
r	blade section radius from center of rotation
R	radius of rotor disk
t	time
T	kinetic energy
U	potential energy
U_{FL}	flutter velocity
V	forward airspeed
W	Loewy's wake weighting function
W_N	finite-wake weighting function
x	non-dimensional distance from mid-chord
Y_N	imaginary part of complex Bessel function
α_n	blade pitch angle due to n^{th} torsional mode
γ_a	vorticity generated by reference airfoil
γ_{nq}	vorticity generated by q^{th} blade in n^{th} revolution
λ	inflow ratio, $\lambda = v_i / \Omega R$
μ	advance ratio, $\mu = V/\Omega R$
ξ	non-dimensional distance from mid-chord

---

[i] Paper presented at 28th European Rotorcraft Forum, Bristol, England, 17-20 September 2002.

[ii] Professor, Department of Aeronautics and Astronautics.

[iii] Lecturer, Department of Aeronautics and Astronautics.

[iv] Associate Professor, Department of Mathematics

ρ	density of air
φ_1	phase angle between initiation of rotation input and arbitrary reference point
φ_2	phase angle between initiation of amplitude input and arbitrary reference point
ψ_q	phase angle by which motion of q^{th} blade leads reference blade
ω	frequency of oscillation
Ω	rotational speed of rotor

Introduction

The conventional method for designing a rotor blade to be free of flutter throughout the helicopter's flight regime is to design the blade so that aerodynamic center (a.c.), elastic axis (e.a.) and blade center of gravity (c.g.) are coincident and located at the quarter-chord. The practice of designing rotor blade c.g. to be coincident at the quarter chord with the elastic axis and concurrent with the a.c. pays off by decoupling the equations used in two-dimensional unsteady aerodynamic theory. While this assures freedom from flutter, it adds constraints on rotor blade design, not usually followed in fixed wing design. Designing a wing such that c.g. and a.c. are coincident at the quarter chord costs weight. It also, if strictly followed, rules out use of a flap which causes the a.c. to move with flap angle. It also restricts use of camber which moves the a.c. aft.

Loewy's (Ref 1) 2-D unsteady aerodynamic theory as amended by Jones and Rao (Ref 2) and Hammond (Ref 3) provides a useful tool for examining blade flutter in hover. Extension of their work to a helicopter in forward flight presents a formidable mathematical challenge, and thus at present, there is no accepted theory to completely analyze blade flutter in forward flight. Here, the effect of a shed skewed helical wake would have to be considered and the contribution of each element of that wake on each segment of the blade at each azimuth position accounted for. Currently to meet forward flight blade flutter requirements the rotorcraft manufacturer must rely on: (1) quasi-fixed wing blade flutter analysis, which does not account for the unsteady contribution of the wake below the rotor; and (2) costly rotor whirl tests at normal and overspeed conditions, which while providing information in regard to blade flutter, do not accurately simulate either blade dynamics or unsteady aerodynamics in forward flight.

However, closer examination of the problem reveals that it is possible to make several simplifying assumptions that make the forward flight flutter problem tractable. In particular, it is assumed at the onset of flutter that oscillations begin to build up prior to the blade reaching a critical azimuth position, then decay as the blade moves beyond this point. Shipman and Wood (Ref 4) provide the basis for the analysis. A description of the mathematical model, formulation, and the results that are obtained are the subject of this paper. The paper also includes a fully worked out numerical example using the UH-60 rotor blade to illustrate the method complete with results.

Theoretical Analysis

Approach to the Problem

Consider a rotary-wing aircraft in steady-state level flight. We examine the unsteady aerodynamics acting on an advancing blade. The basic assumptions incorporated are as follows:

1. Two-dimensional, inviscid, incompressible potential flow.
2. Respective layers of the wake are two-dimensionalized and treated as parallel horizontal sheets.
3. In forward flight, each blade of the rotor will respond in the same manner as every other blade.
4. The most critical azimuth position of the blade in forward flight for the onset of flutter is at $\psi = 90^{\circ}$.
5. At the onset of blade flutter oscillations will begin to build up prior to the blade reaching the critical azimuth position, and these oscillations will decay as the blade moves beyond the critical azimuth position.

At a specified radial location r on the blade, the local tangential velocity would be given by

$$U_t(r) = \Omega r + V \sin\psi$$

If it is assumed that the flutter speed for this blade segment is such that

$$U_{FL}(r) < \Omega r + V,$$

then during each blade revolution the blade segment at r will experience velocities, which will increase to the flutter speed and beyond, then return through the flutter boundary to lower airspeeds. Extending this concept to both blade azimuth position and radial position, we observe that the blade tangential velocity at a given radial position will exceed the flutter speed in some region of rotor azimuth position if

$$V \sin\psi > U_{FL}(r) - \Omega r\ .$$

An example of this region is shown in Fig. 1.

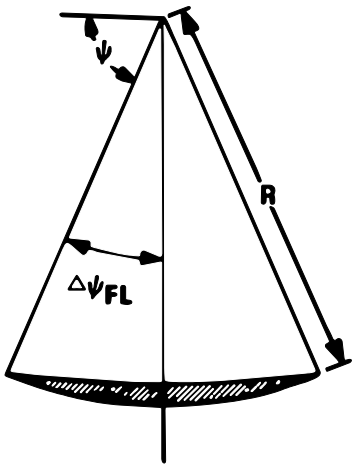

Figure 1. Unstable region encountered by advancing blade.

It should be noted that all points within the shaded region of Fig. 1 will experience negative damping. This negative damping will tend to cause blade motion to grow. Also, in the region of $\psi \leq \pi/2 - \Delta\psi_{FL}$, the damping will decrease as ψ approaches $(\pi/2 - \Delta\psi_{FL})$, whereas in the region $\psi \geq \pi/2 + \Delta\psi_{FL}$, damping will be positive and will increase so that a blade instability would tend to die out.

Consider the effect of this variation in damping on an outboard portion of the advancing blade. It is expected that damping would decrease as the blade approaches $\psi = 90^\circ$, and the amplitude of oscillations would build up. Conversely, as the blade advanced beyond $\psi = 90^\circ$ damping would increase, and there would be a corresponding decrease in blade vibratory amplitude. This build-up and decay of blade amplitude would result in a distribution of shed vorticity as shown by Fig. 2. Here, we observe that timewise variations in amplitude of blade vibrations have resulted in spacewise variations in shed vorticity. Since we have assumed steady-state flight, each blade would shed similar segments of vorticity for each revolution. These vortex segments constitute the wake that will be treated in this analysis.

Based on the foregoing, the bound vorticity on the airfoil can be expressed as the product of a function of chordwise position, a decay function, and a harmonic function of time[v]. We write the incremental bound vorticity as

$$\gamma_a = \bar{\gamma}_a(x) f(\xi_0) e^{i(\omega t + \phi)}$$

where $f(\xi_0)$ is an assumed decay function centered about $\xi_0 = 0$. The limiting case of constant-strength shed vorticity such as considered by Theodorsen (Ref 6) and Loewy (Ref 1) for their analyses, is simply achieved by taking $f(\xi_0) = 1$.

When the inflow velocity through the rotor is small, the shed vorticity remains close to the rotor and the wakes shed from each blade during several previous passes as well as the present pass must be considered. The build-up and decay of vorticity occurs within a double azimuth angle on either side of $\psi = 90^\circ$. The solid lines of Fig. 3 indicate this region of the wake. In this region the azimuth angle between a shed vortex filament and the reference blade may be ignored. The tip does not move very far from the vertical plane shown in Fig. 3 and so its path may be taken to lie in this plane.

Combining the vorticity segments given in Fig. 2, the resulting wake pattern is shown in Fig. 4. With the mathematical model defined, the problem now is to determine the pressure difference across the airfoil due to the vorticity shed in the wake, and consequently to determine the unsteady lift and moment acting on the airfoil.

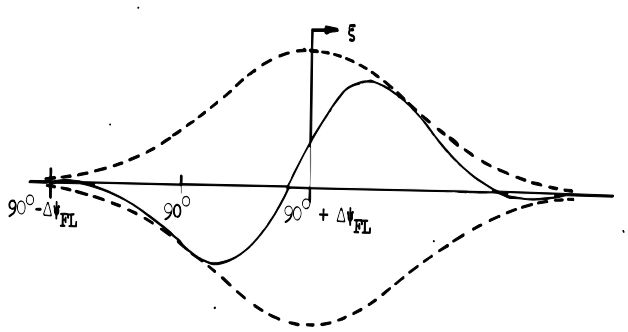

Figure 2. Distribution of shed vorticity in unstable region.

Aerodynamic Forces and Lift Deficiency Functions

Theodorsen (Ref 6) developed the equations for the unsteady aerodynamic forces for fixed-wing aircraft by considering a wing oscillating in simple harmonic motion at frequency ω. The unsteady forces per unit span are given by

$$L' = \pi\rho b^3\omega^2\left\{L_h\frac{h}{b} + \left[L_\alpha - \left(\frac{1}{2} + a\right)L_h\right]\alpha\right\}$$

[v] W. P. Jones (Ref. 5) first treated the case of an oscillating airfoil where the strength of the airfoil's motion was allowed to grow or decay exponentially with time. As the buildup or decay rate approached zero, Jones' lift deficiency function approached that of Theodorsen (Ref 6).

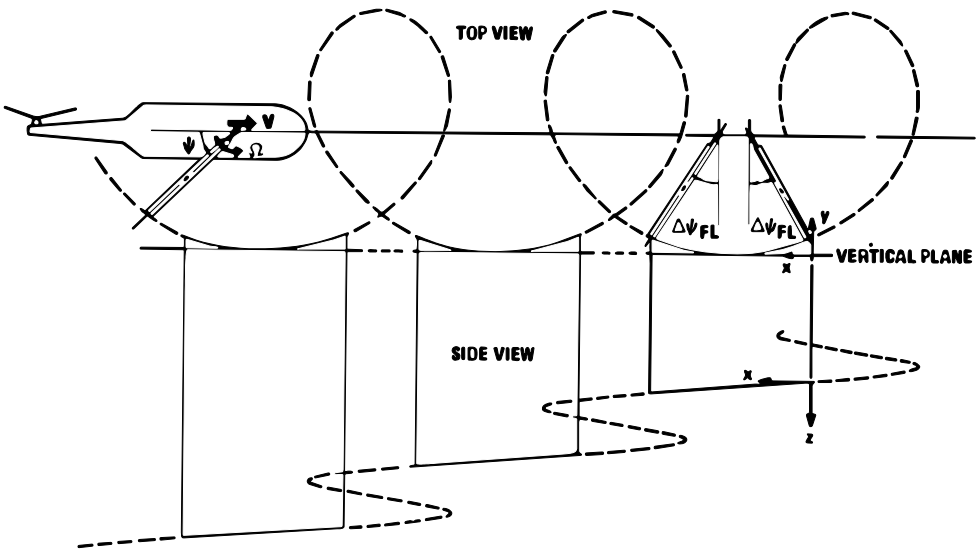

Figure 3. Development of skewed helical wake.

$$M' = \pi\rho b^4\omega^2\left\{\left[M_h - \left(\frac{1}{2}+a\right)L_h\right]\frac{h}{b} + \left[M_\alpha - \left(\frac{1}{2}+a\right)\left(L_\alpha + M_h\right) + \left(\frac{1}{2}+a\right)^2 L_h\right]\alpha\right\}$$

where

$$L_h = 1 - \frac{2i}{k}C(k)$$

$$L_\alpha = \frac{1}{2} - \frac{2i}{k}\left[\frac{1}{2} + \left(1 - \frac{i}{k}\right)C(k)\right]$$

$$M_h = \frac{1}{2}$$

$$M_\alpha = \frac{3}{8} - \frac{i}{k}$$

The term $C(k)$ is Theodorsen's well-known lift deficiency function defined by

$$C(k) = \frac{H_1^{(2)}}{H_1^{(2)} + iH_0^{(2)}}$$

where $H_n^{(2)} = J_n - iY_n$ is the Hankel function of the second kind of order n evaluated at reduced frequency $k = \omega b/V$.

Loewy developed the unsteady aerodynamic forces for a rotor in hover by accounting for the layers of shed vorticity generated by the previous blades in the same revolution and all blades in the previous revolutions. His equations were analogous to Theodorsen's, but included a modified lift deficiency function. Loewy's lift deficiency function is defined by

$$C'(k,h,m) = \frac{H_1^{(2)}(k) + 2J_1(k)W(k,h,m)}{H_1^{(2)}(k) + iH_0^{(2)}(k) + 2\left(J_1(k) + iJ_0(k)\right)W(k,h,m)}$$

where

$$W(k,h,m) = \frac{1}{e^{kh}e^{i2\pi m} - 1},$$

and is evaluated at reduced frequency (k), wake spacing ($h = 2\pi V/bQ\Omega$) and frequency ratio ($m = \omega/\Omega$).

A Theory for Forward Flight

Shipman and Wood, using the theory described in the section on Approach to the Problem, developed their equation for the unsteady forces in forward flight that are analogous to Theodorsen and Loewy, but modified the lift deficiency function to account for the helicopter's forward speed (advance ratio) and the build-up and decay function associated with the advancing blade illustrated in Fig. 4. The forward flight lift deficiency function is defined by

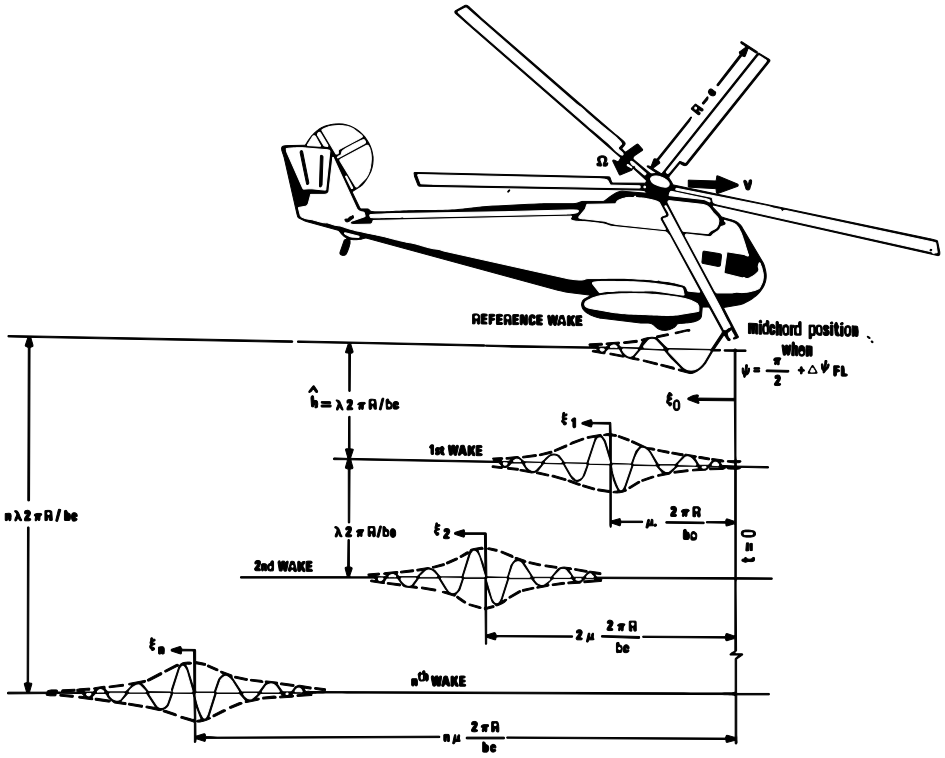

Figure 4. Two-dimensional wake model for forward flight.

$$C'(k,h,m) = \frac{\begin{array}{c} H_1^{(2)}(k) + \Delta F_2(k) + \Delta F_4(k) \\ + 2J_1(k)\left[W(k,h,m) + \Delta W(k,h,m)\right] \end{array}}{\begin{array}{c} H_1^{(2)}(k) + iH_0^{(2)}(k) + \Delta F_3(k) \\ + 2\left(J_1(k) + iJ_0(k)\right)\left[W(k,h,m) + \Delta W(k,h,m)\right] \end{array}}$$

where

$$\Delta F_2(k) = -\frac{2}{\pi}\int_1^\infty \left[f(y) - 1 - \frac{1}{ik}\frac{df}{dy} \right] \frac{ye^{-iky}}{\sqrt{y^2-1}}\, dy$$

$$\Delta F_3(k) = -\frac{2}{\pi}\int_1^\infty \left[f(y) - 1 - \frac{1}{ik}\frac{df}{dy} \right] \left(\sqrt{\frac{y+1}{y-1}} \right) e^{-iky}\, dy$$

$$\Delta F_4(k) = -\frac{2}{\pi}\int_1^\infty \left[\frac{df}{dy} - \frac{1}{ik}\frac{d^2f}{dy^2} \right] \left[y - \sqrt{y^2-1} \right] e^{-iky}\, dy$$

$$\Delta W(k,h,m) = \sum_{n=1}^{\infty} e^{-knh} e^{iknm} \times \left[f(-nm - inh) - 1 - \frac{1}{ik}\frac{df(-nm-inh)}{dy} \right]$$

where $f(y)$ is the assumed decay function[vi].

[vi] The forward flight lift deficiency function described and applied in this paper is similar to that of Shipman and Wood (Ref 4), except the decay function has been modified to eliminate a singularity problem.

UH-60 Blade Sample Problem

Using the forward flight lift deficiency function, a sample numerical problem will now be presented. The flutter determinant for the blade is repeatedly solved in the conventional manner to obtain the blade flutter speed. (See Scanlan and Rosenbaum, Ref 7). But here the newly proposed lift deficiency function is applied. UH-60 blade parameters are used in the sample problem in deference to the extensive database now available for this blade. However, for the demonstration analysis the UH-60 blade will be modified to make it "flutter susceptible". This is achieved by moving the chordwise position of the blade c.g. aft while keeping its elastic axis at the quarter chord. This also introduces flap torsion coupling, a desirable feature for a sample problem of this type.

For the numerical example, the blade is divided into radial segments in the usual manner with unsteady aerodynamics applied to the blade at each panel point. Included in the analysis are a rigid flapping mode, two flapwise bending modes and the blade's first and second torsion mode. Results of the forward flight analysis are compared with baseline values obtained from locking the blade at the 90-degree azimuth position and solving the flutter problem, similar to a fixed wing case with Theodorsen lift

deficiency values, yet allowing radial velocity to vary with span as in the case of the tangential velocity of a rotor blade in forward flight, $\psi = 90^{\circ}$.

Blade Frequencies and Mode Shapes

Characteristics of the UH-60 rotor blade are given in Table 1. Three flapwise bending modes with natural frequencies of 1.035Ω, 2.81Ω and 5.19Ω are incorporated in the flutter analysis together with two torsion modes. The two torsion modes occur at 4.3Ω and 11.0Ω, respectively.

Table 1. Characteristics of UH-60 rotor blade

Parameter	Value	Units
b	4	blades
m	0.52	lb/in.
c	1.73	ft
I_α	2.55	lb in.
R	26.83	ft
e	2.334	ft
e.a.	25% chord	
$x_{c.g.}$	variable	
Ω	258	rpm
ΩR	725	ft/s

Blade bending frequencies and mode shapes used in the present sample analysis were determined by a simplified method made possible by assuming a uniform stiffness and mass distribution for the problem. This makes it possible to simplify the present sample problem by shortcutting a more exact and detailed analysis that would be required to account for such details as local changes in stiffness and mass distribution due to blade features such as doublers near the blade root and outboard blade balance weights near the tip.

The shortcut method for determining frequencies is that by Yntema in NACA TN 3459 (Ref 8). Given the natural frequencies, corresponding non-rotating mode shapes can then be obtained from the well-known report (Ref 9) by Young and Felgar. Yntema's key assumption is that non-rotating mode shapes are very close approximations to rotating mode shapes. Fig 5 , taken from Yntema's report, compares rotating and non-rotating mode shapes for the first three bending modes of a pinned-free beam to validate this assumption.

In Ref 8, Yntema notes that an exact value for the nth bending frequency of a beam rotating at any rotational speed, Ω, can be found if the n^{th} natural bending mode shape is known for this value of rotational speed. He obtains his frequency equation *by equating the kinetic energy at zero displacement to the potential energy of both the bending and centrifugal forces at maximum displacement for vibration perpendicular to the plane of rotation.*

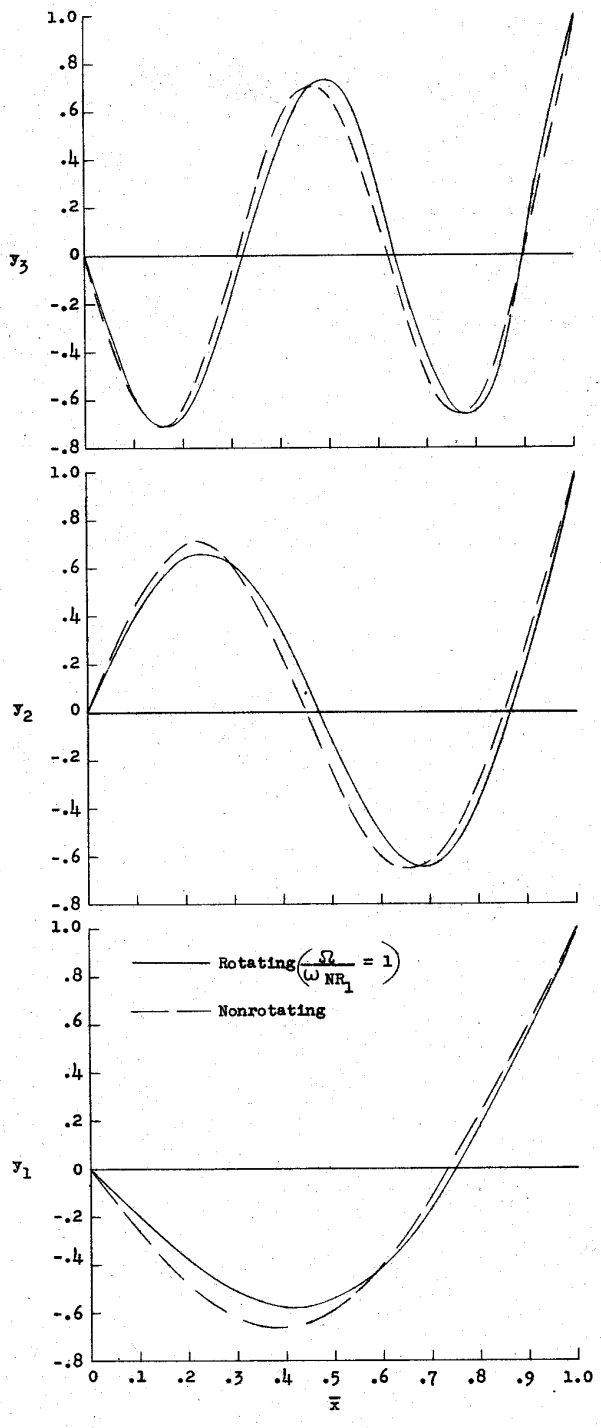

Fig. 5. Comparison of bending modes of a rotating and nonrotating uniform hinged-free beam.

$$\omega_{R_n}^2 = \frac{\int_0^l EIy_n''^2\,dx}{\int_0^l my_n^2\,dx} + \frac{\int_0^l T_1 y_n'^2\,dx}{\int_0^l my_n^2\,dx} \qquad (1)$$

where *n* refers to mode of vibration and

$$T_1 = \int_x^l (\eta + e) m\, d\eta$$

He goes on to point out that while the rotating mode shape is unknown, a close approximation to the rotating natural frequency can be obtained by making use of *Rayleigh's Principle* and using the non-rotating beam mode shape in equation (1). The report states that the non-rotating mode shape is consistent with the constraints of the system (in this case a pinned-free beam). If the n^{th} mode of the non-rotating Y_n is substituted into equation (1), the first term becomes exactly the square of the bending frequency of the non-rotating beam. By denoting the ratio in the second term by K_n , a Southwell coefficient, the form of the frequency equation becomes:

$$\omega_{R_n}^2 = \omega_{NR_n}^2 + K_n \Omega^2$$

To account for blade offset, e, subdivide K_n into two independent parts:

$$K_n = K_{0_n} + K_{1_n} e$$

where K_{0n} is referred to as the zero-offset Southwell coefficient and K_{1n} is referred to as the offset-correction factor for the Southwell coefficient. As is frequently done it is convenient to write the square of the non-rotating frequency in terms of a non-rotating-beam frequency coefficient, a_n , and the mass and stiffness of the beam as:

$$\omega_{NR_n}^2 = a_n^2 \frac{EI_0}{m_0 l^4}$$

Putting this all together yields

$$\omega_{R_n}^2 = a_n^2 \frac{EI_0}{m_0 l^4} + \left(K_{0_n} + K_{1_n} e\right)\Omega^2 \qquad (6)$$

Yntema's report (Ref 8) gives charts that provide a_n , K_{0n} and K_{1n} which, in conjunction with the mass and stiffness of the beam at the root, the length of the beam, the hinge offset, and the rotational speed, permit rapid estimation of the first three bending frequencies of rotating beams with hinged or cantilevered root-end support. As previously noted, once the frequencies have been found, the rotating beam mode shapes can then be approximated by non-rotating mode shapes which are defined for every two percent of the beam's length by the detailed report by Young and Felgar (Ref 9).

Equations of Motion Using Normal Modes

The method of analysis for flutter of a rotor blade parallels that given by Scanlan and Rosenbaum (Ref. 7) for flutter analysis of an airplane wing. There is a fundamental difference in the lift deficiency function as has been already described. For small oscillations of a conservative system, the motion of the system can be considered as superposition of the natural modes of vibration.

The problem as considered here is three-dimensional only to the extent that the spanwise variation of mass, geometry, and mode shape is taken into account. The aerodynamic forces and moments are given by strip theory for infinite-aspect-ratio incompressible flow. It has been found that a reasonable representation of the flutter condition can be obtained by considering the motion of the system a superposition of the fundamental uncoupled bending modes and uncoupled torsion modes of the rotor blade. A basic assumption is that aerodynamic forces and moments do not change the shape of the uncoupled modes of vibration of the rotor blade itself.

Normal Coordinates

With the rotor blade free vibration problem solved, we present the bending deflection as

$$h(x,t) = \sum_{n=1}^{N} f_n(x) q_n(t)$$

where $f_n(x)$ is the characteristic function (mode shape) for the n^{th} vertical bending mode of the rotor blade. The quantities $q_n(t)$ can be considered as weighting functions for each mode that contributes to the deflection. They are called the normal coordinates since they can be shown to reduce the kinetic and potential energy expressions to sums of squares of the coordinates with no cross product terms.

The corresponding torsional deflection of the rotor blade can be written in terms of the blade torsion modes as

$$\alpha(x,t) = \sum_{n=1}^{N} F_n(x) q_n(t)$$

where $F_n(x)$ is the characteristic function of the n^{th} torsional mode of the rotor blade and $q_n(t)$ is the corresponding normal coordinate. Consider the 5 D.O.F. case where we have three bending modes and

two torsion modes. The bending and torsional deflections can be written as

$$h(x,t) = h_1(t)f_1(x) + h_2(t)f_2(x) + h_3(t)f_3(x)$$

and

$$\alpha(x,t) = \alpha_1(t)F_1(x) + \alpha_2(t)F_2(x)$$

where

$f_1(x)$ = 1st vertical bending mode
$f_2(x)$ = 2nd vertical bending mode
$f_3(x)$ = 3rd vertical bending mode
$F_1(x)$ = 1st torsion mode
$F_2(x)$ = 2nd torsion mode

Lagrange's equation is given as

$$\frac{d}{dt}\left(\frac{\partial T}{\partial \dot{q}_n}\right) - \frac{\partial T}{\partial q_n} + \frac{\partial U}{\partial q_n} + \frac{\partial D}{\partial \dot{q}_n} = Q_n$$

where $T \equiv$ kinetic energy, $U \equiv$ potential energy, $D \equiv$ dissipation function, and $Q_n \equiv$ generalized force. For the 5 D.O.F. case,

$$T = \frac{1}{2}M_1\dot{h}_1^2 + \frac{1}{2}M_2\dot{h}_2^2 + \frac{1}{2}M_3\dot{h}_3^2 + \frac{1}{2}I_{\alpha_1}\dot{\alpha}_1^2 + \frac{1}{2}I_{\alpha_2}\dot{\alpha}_2^2 + S_{\alpha_{11}}\dot{h}_1\dot{\alpha}_1 + S_{\alpha_{12}}\dot{h}_1\dot{\alpha}_2 + S_{\alpha_{21}}\dot{h}_2\dot{\alpha}_1 + S_{\alpha_{22}}\dot{h}_2\dot{\alpha}_2 + S_{\alpha_{31}}\dot{h}_3\dot{\alpha}_1 + S_{\alpha_{32}}\dot{h}_3\dot{\alpha}_2$$

$$U = \frac{1}{2}M_1\omega_{h_1}^2h_1^2 + \frac{1}{2}M_2\omega_{h_2}^2h_2^2 + \frac{1}{2}M_3\omega_{h_3}^2h_3^2 + \frac{1}{2}I_{\alpha_1}\omega_{\alpha_1}^2\alpha_1^2 + \frac{1}{2}I_{\alpha_2}\omega_{\alpha_2}^2\alpha_2^2$$

$$D = \frac{M_1g_{h_1}\omega_{h_1}^2\dot{h}_1^2}{2\omega} + \frac{M_2g_{h_2}\omega_{h_2}^2\dot{h}_2^2}{2\omega} + \frac{M_3g_{h_3}\omega_{h_3}^2\dot{h}_3^2}{2\omega} + \frac{I_{\alpha_1}g_{\alpha_1}\omega_{\alpha_1}^2\dot{\alpha}_1^2}{2\omega} + \frac{I_{\alpha_2}g_{\alpha_2}\omega_{\alpha_2}^2\dot{\alpha}_2^2}{2\omega}$$

and the generalized forces are defined as

$$Q_{h_1} = \pi\rho\omega^2\left(A_{11}h_1 + A_{12}h_2 + A_{13}h_3 + A_{14}\alpha_1 + A_{15}\alpha_2\right)$$
$$Q_{h_2} = \pi\rho\omega^2\left(A_{21}h_1 + A_{22}h_2 + A_{23}h_3 + A_{24}\alpha_1 + A_{25}\alpha_2\right)$$
$$Q_{h_3} = \pi\rho\omega^2\left(A_{31}h_1 + A_{32}h_2 + A_{33}h_3 + A_{34}\alpha_1 + A_{35}\alpha_2\right)$$
$$Q_{\alpha_1} = \pi\rho\omega^2\left(A_{41}h_1 + A_{42}h_2 + A_{43}h_3 + A_{44}\alpha_1 + A_{45}\alpha_2\right)$$
$$Q_{\alpha_2} = \pi\rho\omega^2\left(A_{51}h_1 + A_{52}h_2 + A_{53}h_3 + A_{54}\alpha_1 + A_{55}\alpha_2\right)$$

The expressions for aerodynamic terms, A_{ij}, are

$$A_{11} = \int_0^l b^2[f_1(x)]^2 L_h\,dx$$
$$A_{12} = \int_0^l b^2 f_1(x) f_2(x) L_h\,dx$$
$$A_{13} = \int_0^l b^2 f_1(x) f_3(x) L_h\,dx$$
$$A_{14} = \int_0^l b^2 f_1(x) F_1(x)\left[L_\alpha - \left(\frac{1}{2}+a\right)L_h\right]dx$$
$$A_{15} = \int_0^l b^2 f_1(x) F_2(x)\left[L_\alpha - \left(\frac{1}{2}+a\right)L_h\right]dx$$
$$A_{21} = \int_0^l b^2 f_2(x) f_1(x) L_h\,dx = A_{12}$$
$$A_{22} = \int_0^l b^2[f_2(x)]^2 L_h\,dx$$
$$A_{23} = \int_0^l b^2 f_2(x) f_3(x) L_h\,dx$$
$$A_{24} = \int_0^l b^2 f_2(x) F_1(x)\left[L_\alpha - \left(\frac{1}{2}+a\right)L_h\right]dx$$
$$A_{25} = \int_0^l b^2 f_2(x) F_2(x)\left[L_\alpha - \left(\frac{1}{2}+a\right)L_h\right]dx$$
$$A_{31} = \int_0^l b^2 f_3(x) f_1(x) L_h\,dx = A_{13}$$
$$A_{32} = \int_0^l b^2 f_3(x) f_2(x) L_h\,dx = A_{23}$$
$$A_{33} = \int_0^l b^2[f_3(x)]^2 L_h\,dx$$
$$A_{34} = \int_0^l b^2 f_3(x) F_1(x)\left[L_\alpha - \left(\frac{1}{2}+a\right)L_h\right]dx$$
$$A_{35} = \int_0^l b^2 f_3(x) F_2(x)\left[L_\alpha - \left(\frac{1}{2}+a\right)L_h\right]dx$$
$$A_{41} = \int_0^l b^3 F_1(x) f_1(x)\left[M_h - \left(\frac{1}{2}+a\right)L_h\right]dx$$
$$A_{42} = \int_0^l b^3 F_1(x) f_2(x)\left[M_h - \left(\frac{1}{2}+a\right)L_h\right]dx$$
$$A_{43} = \int_0^l b^3 F_1(x) f_3(x)\left[M_h - \left(\frac{1}{2}+a\right)L_h\right]dx$$
$$A_{44} = \int_0^l b^4[F_1(x)]^2\left[M_\alpha - \left(\frac{1}{2}+a\right)(L_\alpha + M_h) + \left(\frac{1}{2}+a\right)^2 L_h\right]dx$$
$$A_{45} = \int_0^l b^4 F_1(x) F_2(x)\left[M_\alpha - \left(\frac{1}{2}+a\right)(L_\alpha + M_h) + \left(\frac{1}{2}+a\right)^2 L_h\right]dx$$
$$A_{51} = \int_0^l b^3 F_2(x) f_1(x)\left[M_h - \left(\frac{1}{2}+a\right)L_h\right]dx$$

$$A_{52} = \int_0^l b^3 F_2(x) f_2(x) \left[M_h - \left(\frac{1}{2} + a \right) L_h \right] dx$$

$$A_{53} = \int_0^l b^3 F_2(x) f_3(x) \left[M_h - \left(\frac{1}{2} + a \right) L_h \right] dx$$

$$A_{54} = \int_0^l b^4 F_2(x) F_1(x) \left[M_\alpha - \left(\frac{1}{2} + a \right) (L_\alpha + M_h) + \left(\frac{1}{2} + a \right)^2 L_h \right] dx = A_{45}$$

$$A_{55} = \int_0^l b^4 [F_2(x)]^2 \left[M_\alpha - \left(\frac{1}{2} + a \right) (L_\alpha + M_h) + \left(\frac{1}{2} + a \right)^2 L_h \right] dx$$

The generalized masses of the three bending modes and two generalized torsion modes can be written as

$$M_1 = \int_0^l m(x) [f_1(x)]^2 \, dx$$

$$M_2 = \int_0^l m(x) [f_2(x)]^2 \, dx$$

$$M_3 = \int_0^l m(x) [f_3(x)]^2 \, dx$$

$$I_{\alpha_1} = \int_0^l I_\alpha(x) [F_1(x)]^2 \, dx$$

$$I_{\alpha_2} = \int_0^l I_\alpha(x) [F_2(x)]^2 \, dx$$

The static unbalance terms are defined as

$$S_{\alpha_{11}} = \int_0^l S_\alpha(x) f_1(x) F_1(x) dx$$

$$S_{\alpha_{12}} = \int_0^l S_\alpha(x) f_1(x) F_2(x) dx$$

$$S_{\alpha_{21}} = \int_0^l S_\alpha(x) f_2(x) F_1(x) dx$$

$$S_{\alpha_{22}} = \int_0^l S_\alpha(x) f_2(x) F_2(x) dx$$

$$S_{\alpha_{31}} = \int_0^l S_\alpha(x) f_3(x) F_1(x) dx$$

$$S_{\alpha_{32}} = \int_0^l S_\alpha(x) f_3(x) F_2(x) dx$$

First it is noted that the kinetic energy equation is only a function of the derivative of the generalized displacement ($\dot{h}_n$ or $\dot{\alpha}_n$). Thus, Lagrange's equation reduces to

$$\frac{d}{dt}\left(\frac{\partial T}{\partial \dot{q}_n} \right) + \frac{\partial U}{\partial q_n} + \frac{\partial D}{\partial \dot{q}_n} = Q_n$$

Applying Lagrange's equation to each of the 5 D.O.F. yields the following five equations:

$$M_1 \ddot{h}_1 + S_{\alpha_{11}} \ddot{\alpha}_1 + S_{\alpha_{12}} \ddot{\alpha}_2 + M_1 \omega_{h_1}^2 h_1 + \frac{M_1 \omega_{h_1}^2 g_{h_1}}{\omega} \dot{h}_1 = Q_{h_1}$$

$$M_2 \ddot{h}_2 + S_{\alpha_{21}} \ddot{\alpha}_1 + S_{\alpha_{22}} \ddot{\alpha}_2 + M_2 \omega_{h_2}^2 h_2 + \frac{M_2 \omega_{h_2}^2 g_{h_2}}{\omega} \dot{h}_2 = Q_{h_2}$$

$$M_3 \ddot{h}_3 + S_{\alpha_{31}} \ddot{\alpha}_1 + S_{\alpha_{32}} \ddot{\alpha}_2 + M_3 \omega_{h_3}^2 h_3 + \frac{M_3 \omega_{h_3}^2 g_{h_3}}{\omega} \dot{h}_3 = Q_{h_3}$$

$$I_{\alpha_1} \ddot{\alpha}_1 + S_{\alpha_{11}} \ddot{h}_1 + S_{\alpha_{21}} \ddot{h}_2 + S_{\alpha_{31}} \ddot{h}_3 + I_{\alpha_1} \omega_{\alpha_1}^2 \alpha_1 + \frac{I_{\alpha_1} \omega_{\alpha_1}^2 g_{\alpha_1}}{\omega} \dot{\alpha}_1 = Q_{\alpha_1}$$

$$I_{\alpha_2} \ddot{\alpha}_2 + S_{\alpha_{12}} \ddot{h}_1 + S_{\alpha_{22}} \ddot{h}_2 + S_{\alpha_{32}} \ddot{h}_3 + I_{\alpha_2} \omega_{\alpha_2}^2 \alpha_2 + \frac{I_{\alpha_2} \omega_{\alpha_2}^2 g_{\alpha_2}}{\omega} \dot{\alpha}_2 = Q_{\alpha_2}$$

If simple harmonic motion is assumed, that is: $\ddot{h}_n = -\omega^2 h_n$; $\dot{h}_n = i\omega h_n$; $\ddot{\alpha}_n = -\omega^2 \alpha_n$; and $\dot{\alpha}_n = i\omega\alpha_n$, and the expressions for Q_{h_n} and Q_{α_n} are substituted into the equations of motion, the results are

$$\left[\pi\rho A_{11} + M_1 - M_1 \left(1 + i g_{h_1}\right) \left(\frac{\omega_{h_1}}{\omega} \right)^2 \right] h_1 + \left(\pi\rho A_{12}\right) h_2 + \left(\pi\rho A_{13}\right) h_3 + \left(\pi\rho A_{14} + S_{\alpha_{11}}\right) \alpha_1 + \left(\pi\rho A_{15} + S_{\alpha_{12}}\right) \alpha_2 = 0$$

$$\left(\pi\rho A_{21}\right) h_1 + \left[\pi\rho A_{22} + M_2 - M_2 \left(1 + i g_{h_2}\right) \left(\frac{\omega_{h_2}}{\omega} \right)^2 \right] h_2 + \left(\pi\rho A_{23}\right) h_3 + \left(\pi\rho A_{24} + S_{\alpha_{21}}\right) \alpha_1 + \left(\pi\rho A_{25} + S_{\alpha_{22}}\right) \alpha_2 = 0$$

$$\left(\pi\rho A_{31}\right) h_1 + \left(\pi\rho A_{32}\right) h_2 + \left[\pi\rho A_{33} + M_3 - M_3 \left(1 + i g_{h_3}\right) \left(\frac{\omega_{h_3}}{\omega} \right)^2 \right] h_3 + \left(\pi\rho A_{34} + S_{\alpha_{31}}\right) \alpha_1 + \left(\pi\rho A_{35} + S_{\alpha_{32}}\right) \alpha_2 = 0$$

$$\left(\pi\rho A_{41} + S_{\alpha_{11}}\right) h_1 + \left(\pi\rho A_{42} + S_{\alpha_{21}}\right) h_2 + \left(\pi\rho A_{43} + S_{\alpha_{31}}\right) h_3 + \left[\pi\rho A_{44} + I_{\alpha_1} - I_{\alpha_1} \left(1 + i g_{\alpha_1}\right) \left(\frac{\omega_{\alpha_1}}{\omega} \right)^2 \right] \alpha_1 + \pi\rho A_{45} \alpha_2 = 0$$

and

$$\left(\pi\rho A_{51} + S_{\alpha_{12}}\right) h_1 + \left(\pi\rho A_{52} + S_{\alpha_{22}}\right) h_2 + \left(\pi\rho A_{53} + S_{\alpha_{32}}\right) h_3 + \pi\rho A_{54} \alpha_1 + \left[\pi\rho A_{55} + I_{\alpha_2} - I_{\alpha_2} \left(1 + i g_{\alpha_2}\right) \left(\frac{\omega_{\alpha_2}}{\omega} \right)^2 \right] \alpha_2 = 0$$

The five equations to the flutter problem can be written in matrix form as shown in Fig. 6. The solution to the flutter problem is found by solving the

$$
\begin{bmatrix}
\left[\pi\rho A_{11}+M_1-M_1\left(1+ig_{h_1}\right)\left(\frac{\omega_{h_1}}{\omega}\right)\right] & \pi\rho A_{12} & \pi\rho A_{13} & \pi\rho A_{14}+S_{\alpha_{11}} & \pi\rho A_{15}+S_{\alpha_{12}} \\
\pi\rho A_{21} & \left[\pi\rho A_{22}+M_2-M_2\left(1+ig_{h_2}\right)\left(\frac{\omega_{h_2}}{\omega}\right)\right] & \pi\rho A_{23} & \pi\rho A_{24}+S_{\alpha_{21}} & \pi\rho A_{25}+S_{\alpha_{22}} \\
\pi\rho A_{31} & \pi\rho A_{32} & \left[\pi\rho A_{33}+M_3-M_3\left(1+ig_{h_3}\right)\left(\frac{\omega_{h_3}}{\omega}\right)\right] & \pi\rho A_{34}+S_{\alpha_{31}} & \pi\rho A_{35}+S_{\alpha_{32}} \\
\pi\rho A_{41}+S_{\alpha_{11}} & \pi\rho A_{42}+S_{\alpha_{21}} & \pi\rho A_{43}+S_{\alpha_{31}} & \left[\pi\rho A_{44}+I_{\alpha_1}-I_{\alpha_1}\left(1+ig_{\alpha_1}\right)\left(\frac{\omega_{\alpha_1}}{\omega}\right)\right] & \pi\rho A_{45} \\
\pi\rho A_{51}+S_{\alpha_{12}} & \pi\rho A_{52}+S_{\alpha_{22}} & \pi\rho A_{53}+S_{\alpha_{32}} & \pi\rho A_{54} & \left[\pi\rho A_{55}+I_{\alpha_2}-I_{\alpha_2}\left(1+ig_{\alpha_2}\right)\left(\frac{\omega_{\alpha_2}}{\omega}\right)\right]
\end{bmatrix}
\begin{bmatrix} h_1 \\ h_2 \\ h_3 \\ \alpha_1 \\ \alpha_2 \end{bmatrix} = 0
$$

Fig. 6 Flutter equations in matrix form.

eignenvalue problem $\left(\overline{A}-IZ\right)X=0$ by arbitrarily letting

$$Z=\left(\frac{\omega_{\alpha_1}}{\omega}\right)^2\left(1+ig\right),$$

which results in

$$
\begin{vmatrix}
\overline{A}_{11}-Z & \overline{A}_{12} & \overline{A}_{13} & \overline{A}_{14} & \overline{A}_{15} \\
\overline{A}_{21} & \overline{A}_{22}-Z & \overline{A}_{23} & \overline{A}_{24} & \overline{A}_{25} \\
\overline{A}_{31} & \overline{A}_{32} & \overline{A}_{33}-Z & \overline{A}_{34} & \overline{A}_{35} \\
\overline{A}_{41} & \overline{A}_{42} & \overline{A}_{43} & \overline{A}_{44}-Z & \overline{A}_{45} \\
\overline{A}_{51} & \overline{A}_{52} & \overline{A}_{53} & \overline{A}_{54} & \overline{A}_{55}-Z
\end{vmatrix} = 0
$$

The non-dimensional determinant elements are defined as

$$\overline{A}_{11}=\left(\frac{\pi\rho A_{11}}{M_1}+1\right)\left(\frac{\omega_{\alpha_1}}{\omega_{h_1}}\right)^2$$

$$\overline{A}_{12}=\left(\frac{\pi\rho A_{12}}{M_1}\right)\left(\frac{\omega_{\alpha_1}}{\omega_{h_1}}\right)^2$$

$$\overline{A}_{13}=\left(\frac{\pi\rho A_{13}}{M_1}\right)\left(\frac{\omega_{\alpha_1}}{\omega_{h_1}}\right)^2$$

$$\overline{A}_{14}=\left(\frac{\pi\rho A_{14}+S_{\alpha_{11}}}{M_1}\right)\left(\frac{\omega_{\alpha_1}}{\omega_{h_1}}\right)^2$$

$$\overline{A}_{15}=\left(\frac{\pi\rho A_{15}+S_{\alpha_{12}}}{M_1}\right)\left(\frac{\omega_{\alpha_1}}{\omega_{h_1}}\right)^2$$

$$\overline{A}_{21}=\left(\frac{\pi\rho A_{21}}{M_2}\right)\left(\frac{\omega_{\alpha_1}}{\omega_{h_2}}\right)^2$$

$$\overline{A}_{22}=\left(\frac{\pi\rho A_{22}}{M_2}+1\right)\left(\frac{\omega_{\alpha_1}}{\omega_{h_2}}\right)^2$$

$$\overline{A}_{23}=\left(\frac{\pi\rho A_{23}}{M_2}\right)\left(\frac{\omega_{\alpha_1}}{\omega_{h_2}}\right)^2$$

$$\overline{A}_{24}=\left(\frac{\pi\rho A_{24}+S_{\alpha_{21}}}{M_2}\right)\left(\frac{\omega_{\alpha_1}}{\omega_{h_2}}\right)^2$$

$$\overline{A}_{25} = \left(\frac{\pi\rho A_{25} + S_{\alpha_{22}}}{M_2}\right)\left(\frac{\omega_{\alpha_1}}{\omega_{h_2}}\right)^2$$

$$\overline{A}_{31} = \left(\frac{\pi\rho A_{31}}{M_3}\right)\left(\frac{\omega_{\alpha_1}}{\omega_{h_3}}\right)^2$$

$$\overline{A}_{32} = \left(\frac{\pi\rho A_{32}}{M_3}\right)\left(\frac{\omega_{\alpha_1}}{\omega_{h_3}}\right)^2$$

$$\overline{A}_{33} = \left(\frac{\pi\rho A_{33}}{M_3} + 1\right)\left(\frac{\omega_{\alpha_1}}{\omega_{h_3}}\right)^2$$

$$\overline{A}_{34} = \left(\frac{\pi\rho A_{34} + S_{\alpha_{31}}}{M_3}\right)\left(\frac{\omega_{\alpha_1}}{\omega_{h_3}}\right)^2$$

$$\overline{A}_{35} = \left(\frac{\pi\rho A_{35} + S_{\alpha_{32}}}{M_3}\right)\left(\frac{\omega_{\alpha_1}}{\omega_{h_3}}\right)^2$$

$$\overline{A}_{41} = \left(\frac{\pi\rho A_{41} + S_{\alpha_{11}}}{I_{\alpha_1}}\right)$$

$$\overline{A}_{42} = \left(\frac{\pi\rho A_{42} + S_{\alpha_{21}}}{I_{\alpha_1}}\right)$$

$$\overline{A}_{43} = \left(\frac{\pi\rho A_{43} + S_{\alpha_{31}}}{I_{\alpha_1}}\right)$$

$$\overline{A}_{44} = \left(\frac{\pi\rho A_{44}}{I_{\alpha_1}} + 1\right)$$

$$\overline{A}_{45} = \left(\frac{\pi\rho A_{45}}{I_{\alpha_1}}\right)$$

$$\overline{A}_{51} = \left(\frac{\pi\rho A_{51} + S_{\alpha_{12}}}{I_{\alpha_2}}\right)\left(\frac{\omega_{\alpha_1}}{\omega_{\alpha_2}}\right)^2$$

$$\overline{A}_{52} = \left(\frac{\pi\rho A_{52} + S_{\alpha_{22}}}{I_{\alpha_2}}\right)\left(\frac{\omega_{\alpha_1}}{\omega_{\alpha_2}}\right)^2$$

$$\overline{A}_{53} = \left(\frac{\pi\rho A_{53} + S_{\alpha_{32}}}{I_{\alpha_2}}\right)\left(\frac{\omega_{\alpha_1}}{\omega_{\alpha_2}}\right)^2$$

$$\overline{A}_{54} = \left(\frac{\pi\rho A_{54}}{I_{\alpha_2}}\right)\left(\frac{\omega_{\alpha_1}}{\omega_{\alpha_2}}\right)^2$$

$$\overline{A}_{55} = \left(\frac{\pi\rho A_{55}}{I_{\alpha_2}} + 1\right)\left(\frac{\omega_{\alpha_1}}{\omega_{\alpha_2}}\right)^2$$

It should be noted that the coefficients of the characteristic equation of the $\left(\overline{A} - IZ\right)$ matrix (a quintic in Z) are complex, and thus the eigenvalues will be complex.

The frequency of oscillation (ω) for each eigenvalue can be found from the real part of Z since the first torsional natural frequency is already known, or

$$\omega_i = \frac{\omega_{\alpha_1}}{\sqrt{\mathrm{Re}(Z)}}$$

The damping coefficient required for flutter to exist (g) for each eigenvalue can be found from the imaginary part of Z, or

$$g_i = \mathrm{Im}(Z)\left(\frac{\omega_i}{\omega_{\alpha_1}}\right)^2$$

If g is negative for the reduced frequency chosen, then damping must be decreased in order to be at the point of instability for flutter to exist. Negative values of g represent the stable, or non-flutter condition. If g is positive, then damping must be increased in order to be at the point of instability for flutter to exist. Positive values of g represent the unstable, or flutter condition. When a plot of g is made against $1/k$, there will be five curves corresponding to the variation of each eigenvalue as the reduced frequency varies. Some of these curves will have only values of g that are negative. These are the non-critical curves and do not influence the flutter solution. However, at least one curve will start with a negative value of g and then at some point cross the abscissa ($1/k$) to a positive value of g. This curve is called the critical curve, and the value of $1/k$ where this curve crosses the abscissa represents the critical flutter speed. The critical flutter speed is found from the relationship

$$U_{FL} = \frac{\omega b}{k_{crit}}$$

where ω is found from the real part of the eigenvalue relationship described above for the critical curve evaluated at the reduced frequency that corresponds to the crossover point (k_{crit}).

Results and Conclusions

This paper has presented a theoretical method for determining rotor blade flutter in forward flight together with a detailed sample problem that treats the bending torsion flutter of a modified UH-60 rotor blade. For the theory a wake model is postulated where it is assumed at the onset of flutter that oscillations begin to build up prior to the blade reaching a critical azimuth position at the $\Psi = 90^o$ position. Oscillations begin to decay as the blade moves past this point.

For the sample problem a flutter determinant has been derived in the manner of Scanlan and Rosenbaum (Ref 7) using normal modes (Ref 10). The determinant is solved repeatedly to obtain the frequency and damping of each blade mode until a flutter speed is found.

Five blade modes are considered in the analysis. These are rigid blade flapping, first and second blade bending modes, and first and second blade torsion modes. To expedite the analysis, Yntema's method (Ref 8) is applied to obtain the first and second blade bending frequencies. Non-rotating mode shapes are taken from Young and Felgar (Ref 9). Torsional mode shapes are from Volkin (Ref 11).

References

1. Loewy, R. G., "A Two-Dimensional Approach to the Unsteady Aerodynamics of Rotary Wings," *Journal of the Aeronautical Sciences*, Vol. 24, Feb. 1957, pp. 82-98.
2. Jones, W. P. and Rao, B. M., "Compressibility Effects on Oscillating Rotor Blades in Hovering Flight," *Volume of Technical Papers on Structural Dynamics and Aeroelasticity Specialist Conference*, New Orleans, LA, April 16-17, 1969.
3. Hammond, C.E., "Compressibility Effects in Helicopter Rotor Blade Flutter," *Ph.D. thesis, Dec. 1969*, Georgia Institute of Technology.
4. Shipman, K. W. and Wood, E. R., "A Two-Dimensional Theory for Rotor Blade Flutter in Forward Flight," *AIAA Journal of Aircraft*, Vol. 8, No. 12, pp. 1008-1015, December 1971.
5. Jones, W. P., "Aerodynamic Forces on Wings in Non-uniform Motion," *Reports. And Memo. 2117*, British Aeronautical Research Council, 1945.
6. Theodorsen, T., "General Theory of Aerodynamic Instability and the Mechanism of Flutter," *NACA Report. 496*, 1935.
7. Scanlan, R. H., and Rosenbaum, R., Introduction to the Study of Aircraft Vibration and Flutter, The Macmillan Co., New York, 1951.
8. Yntema, R. T., "Simplified Procedures and Charts for the Rapid Estimation of Bending Frequencies of Rotating Beams", NACA Technical Note 3459, Langley Field, VA, June 1955.
9. Young, D. and Felgar, R. P., Jr., "Tables of Characteristic Functions Representing Normal Modes of Vibration of a Beam", Bulletin No. 4913, Bureau of Engineering Research, The University of Texas, July, 1949.
10. Young, Dana (of Yale University), "Vibrations of Multi-Degree of Freedom Systems and Continuous Systems", Series of Lectures Given at G.E.'s Engineering Laboratory, Schenectady, NY, February 1955.
11. Volkin, R. S., "Estimation of Rotor Blade Torsional Deformations from Measured Blade Torsion Moments", Thesis for M.S.A.E. Degree, Naval Postgraduate School, Monterey, CA, March 2002.